Journal of ELECTRONIC MATERIALS, Vol. 46, No. 7, 2017
DOI: 10.1007/s11664-017-5442-8

Cellulose Acetate/N-TiO_2 Biocomposite Flexible Films with Enhanced Solar Photochromic Properties

T. RADHIKA,[1,4] K.R. ANJU,[1] M.S. SILPA,[2] R. JOTHI RAMALINGAM,[3,5] and HAMAD A. AL-LOHEDAN[3]

1.—Centre for Materials for Electronics Technology [C-MET], (MeitY), M.G. Kavu P.O., Athani, Thrissur 680581, India. 2.—Department of Bio-Polymer Science, Centre for Biopolymer Science and Technology (CBPST), S. Kalamaseery P.O., Cochin, Kerala 682022, India. 3.—Surfactants Research Chair, Chemistry Department, College of Science, King Saud University, Riyadh 11451, Saudi Arabia. 4.—e-mail: rads12@gmail.com. 5.—e-mail: jrajabathar@ksu.edu.sa

Flexible cellulose acetate/N-TiO_2 nanocomposite films containing various concentrations of nanosized N-TiO_2 and an intelligent methylene blue ink have been prepared by solution casting. The hydrothermally prepared nitrogen-doped titania (N-TiO_2) and the films were characterized in detail. The photochromic properties of the prepared films were investigated under ultraviolet (UV), visible light, and simulated solar irradiation by UV–Vis spectrophotometry. Upon irradiation, the films exhibited rapid photochromic response that was reversible at room temperature. Films with higher content of nano N-TiO_2 showed enhanced decoloration/recoloration under all irradiation conditions, with fast decoloration/recoloration under simulated solar irradiation. These results suggest that the amount of nano N-TiO_2 in the composite, the concentration of methylene blue, and the solvent greatly influence the photochromic properties of the films. Such flexible and transparent cellulose acetate/N-TiO_2 films with enhanced decoloration/recoloration properties under solar irradiation are promising smart materials for use in photoreversible printed electronics applications.

Key words: Cellulose acetate, N-TiO_2, biopolymer, photochromism, nanocomposite, visible light

INTRODUCTION

Photochromic materials have attracted increasing attention owing to their promising applications in a wide variety of fields such as optical displays, data storage, optoelectronic devices, and chemical sensors.[1,2] Specifically, the photochromism of inorganic–organic composite materials has been the subject of intense investigation due to their facile use in practical applications.[3] Although various chromophore compounds have been developed, challenges are still faced in practical applications due to their limitations in terms of reversibility and switching rate.[4] TiO_2 has been extensively studied due to its unique chemical and physical properties, playing an important role in many applications such as photocatalysis, dye-sensitized solar cells, environmental self-cleaning tiles and windows, detoxification of air pollutants, antiseptic paints, chemical sensors, skin cancer treatments, and antifog mirrors.[5,6]

Cellulose can be subject to various types of derivatization to form strong, stable stiff-chain homomolecular structures with film- and hydrogel-forming properties. Therefore, in combination with other, conducting optical materials, cellulose has potential as a stable and robust carrier, matrix, or scaffold component for fabrication of functional materials.[7] Cellulose acetate (CA, ~53% to 56% acetyl group) is the acetate ester of cellulose, a natural biopolymer with many applications such as modern coatings, controlled release, optical films and membranes, as well as in the traditional textile

(Received December 15, 2016; accepted March 4, 2017; published online March 27, 2017)

field in the form of fibers, films, and plastics.[8] Addition of appropriate plasticizers to CA results in a plastic material with excellent transparency and pleasant texture. Cellulose acetate with such a degree of substitution is biodegradable. However, when common plasticizers are substituted by specific esters and other low-molecular-weight components, the resulting plastic material has the same thermoplastic properties but will decompose in soil or water within a few years.[9]

Nanocomposites of these materials have great potential for applications, as they can combine useful chemical, optical, and mechanical properties.[10] Hence, introduction of nanotitania into a cellulosic polymer matrix has been used for modification of the material properties.[11] Therefore, the combination of CA with TiO_2 powder could have further applications. TiO_2 (anatase) is considered to be a good semiconductor photocatalyst because of its excellent photocatalytic activity, UV absorption, robustness, chemical inertness, and ease of deposition, playing a vital role in photocatalytic applications due to its high specific surface area.[12] Therefore, combination of CA with doped titania showing absorption in the visible region could enable devices with interesting properties. Instead of using normal titania, modified TiO_2 can be obtained by adding heteroatoms, e.g., N-TiO_2.[13–15] Inks that, when printed or coated onto a photocatalytic film, change color rapidly and irreversibly upon visible/UV irradiation have been described. Generally, such intelligent inks comprise semiconductor (SC) material, i.e., TiO_2 (anatase), a sacrificial electron donor (SED), a solvent, and a redox dye,[16] being produced in film form for photochromic applications. The intelligent ink used in this work, comprising SC, SED, and a redox dye, was incorporated into a biopolymer–nanocomposite formulation for easy fabrication of photochromic films.[4,17] We report herein a simple method for fabrication of flexible and transparent CA/N-TiO_2 films including an ink with enhanced photochromic properties under visible light and simulated solar irradiation. These films offer rapid solar response and the ability to recover their color completely under normal conditions without additional heating, thereby having great potential for use in photochromic smart windows and rewritable printed electronics devices.

EXPERIMENTAL PROCEDURES

Materials

The chemicals used were metal oxide organic precursor [titanium(IV) butoxide, TBO, AR, Sigma Aldrich], cellulose acetate (CA, Loba Chemie), *N*-cetyl-*N*,*N*,*N*-trimethylammonium bromide (CTAB, Loba Chemie), triethanolamine (TEA), and methylene blue (MB, Merck). Acetic acid (CH_3COOH, Loba Chemie) was used as received.

Preparation of N-TiO_2

N-TiO_2 was prepared via a hydrothermal method. In a typical procedure, titanium(IV) butoxide (TBO) precursor containing urea and surfactant (CTAB) was hydrolyzed with H_2O at TBO:CTAB:urea:distilled H_2O molar ratio of 1:0.1:0.01:100, followed by adjustment to basic pH using ammonia. This was transferred into a Teflon-lined autoclave and placed in an oven at 110°C for 24 h. The white precipitate thus obtained was centrifuged and dried at 60°C to obtain nanosized N-TiO_2. The powder was calcined at 500°C.

Preparation of CA Film

CA film was prepared by a simple solution casting method. About 0.5 g CA was dissolved in acetic acid with constant stirring until it became homogeneous. This solution was poured into a Petri dish and dried at 100°C for 12 h. The dried films were removed from the Petri dish.

Preparation of CA/N-TiO_2 Nanocomposite Photochromic Films

About 0.5 g CA was dissolved in acetic acid with constant stirring. To this solution, N-TiO_2 powder and intelligent ink consisting of MB dye, solvent, and a reducing agent (TEA, ascorbic acid, glycerol, etc.) were added and stirring was continued until the solution became homogeneous. The homogeneous solution was poured into a Petri dish and kept at 60°C for 12 h. The dried films were recovered from the Petri dish.

Material Characterization

The materials were characterized using powder x-ray diffraction analysis (AXS Bruker D5005 x-ray diffractometer), thermogravimetry (TG)-differential scanning calorimetry (DSC), Raman spectroscopy (DSR Raman microscope), Fourier-transform infrared (FT-IR) spectroscopy, diffuse reflectance (DR) UV–Vis spectroscopy (JASCO UV–Vis spectrophotometer V550 ISV469), and scanning electron microscopy (SEM)/transmission electron microscopy (TEM).

Evaluation of Photochromic Properties

The photochromic properties of the CA/N-TiO_2 photochromic films were investigated under UV, visible light, and simulated solar irradiation. The decoloration and recoloration rates of the films were monitored visually as well as by UV–Vis spectroscopy.

RESULTS AND DISCUSSION

N-TiO_2 prepared by the hydrothermal method was characterized in detail using various techniques. The powder XRD pattern of the material is shown in Fig. 1. The XRD pattern clearly showed the characteristic planes of the prepared N-TiO_2 at

2θ = 25.3° (101), 37.9° (004), 48.1° (200), 55.2° (105), and 62.8° (204), with the anatase (101) signal being the most intense. The absence of any other peaks indicates that the N-TiO_2 prepared by the hydrothermal method contained only a single phase. Since the calcination temperature is similar to that of TiO_2, the anatase peak was the most intense peak for the prepared sample.[18,19] Further modification of TiO_2 did not affect the phase. The strong and sharp diffraction peaks indicate good crystallinity of the synthesized material. The thermal characteristics of N-TiO_2 as obtained from TG-DSC analysis are presented in Fig. 2. The weight loss observed up to 400°C is due to evaporation of the surfactant (CTAB) used during the hydrothermal preparation of N-TiO_2. Little weight loss is observed above 500°C, suggesting that the prepared nanomaterial was stable in the temperature range from 500°C to 800°C, with further weight loss being observed above 800°C (Fig. 2). The observed DSC pattern suggests transformation of anatase to rutile TiO_2 when the temperature was increased above 800°C. The DR UV–Vis absorbance spectrum for N-TiO_2 is shown in Fig. 3, consisting of

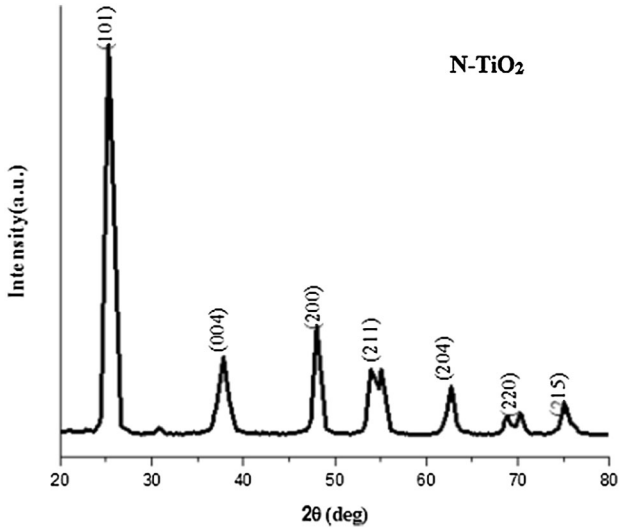

Fig. 1. Powder XRD pattern of N-TiO_2.

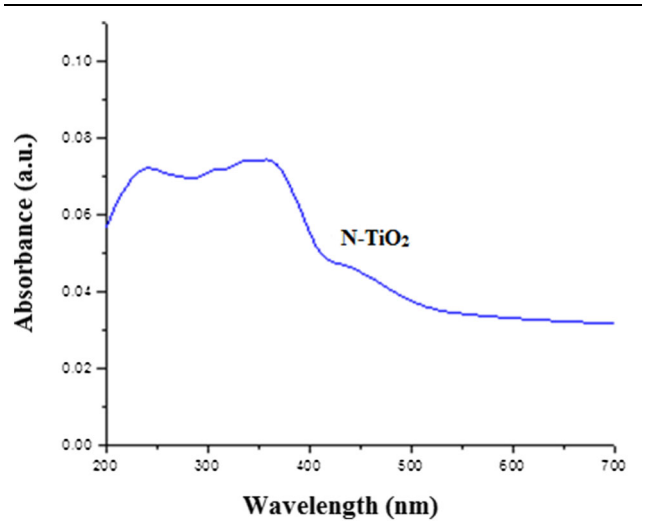

Fig. 3. DR UV–Vis spectrum of N-TiO_2.

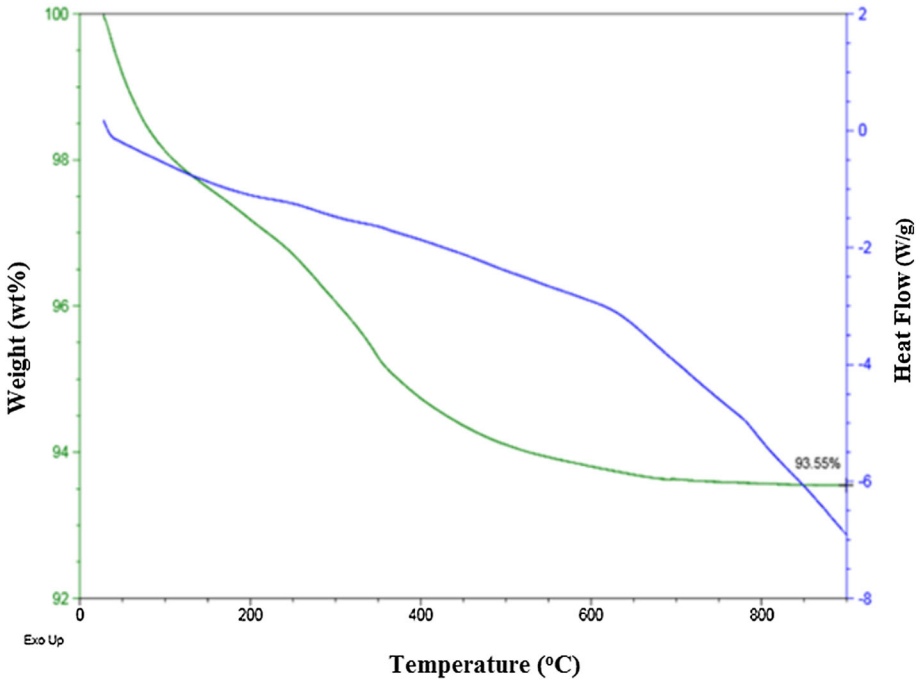

Fig. 2. TG-DSC pattern of N-TiO_2.

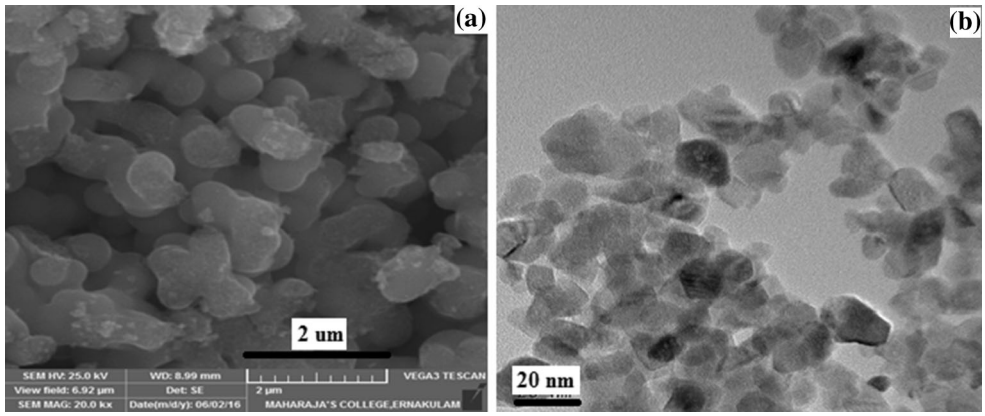

Fig. 4. (a) SEM and (b) TEM micrographs of N-TiO_2.

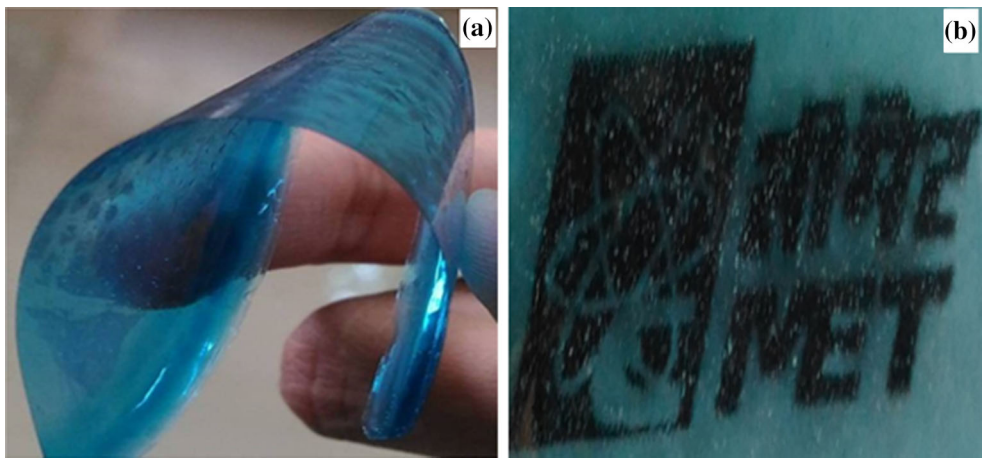

Fig. 5. (a) Flexibility and (b) transparency of the film.

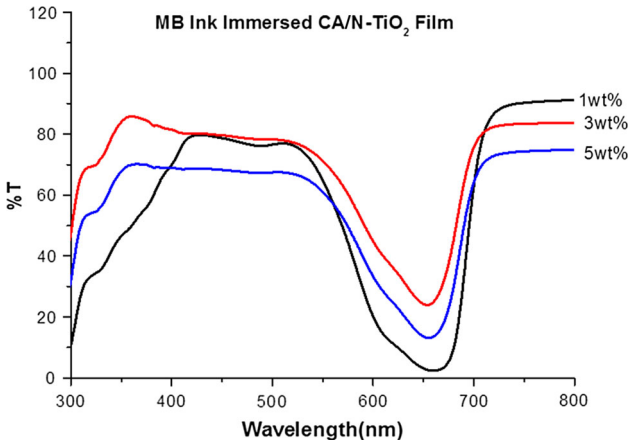

Fig. 6. Transmittance spectra of CA/N-TiO_2 films.

a broad intense absorption with λ_{max} around 421 nm (corresponding to bandgap energy of 2.9 eV calculated from the formula $\lambda = 1239.8/E_g$) due to charge transfer from the valence band formed by 2*p* orbitals of oxygen anions (O^{2-}) in the metal oxide to the conduction band formed by 3*d* t_{2g} orbitals of Ti cations. The spectrum shows a red-shift towards the visible region. Thus, the N-TiO_2 shows a prominent change in the band edge from the UV to visible region (2.9 eV to 2.3 eV). The wavelength response range of this nanosized N-TiO_2 therefore extends into the visible region, corresponding to an increased number of photogenerated electrons and holes that can participate in photosensitive effects.[20] Scanning and transmission electron micrographs revealed that both the ceramic and modified ceramic exhibited uniform spherical shape morphology (Fig. 4a, b).

Table I. Effect on transparency of nanotitania doping of cellulose acetate

Material	Transparency (%)
CA	100
CA/1N-TiO_2	90
CA/3N-TiO_2	83
CA/5N-TiO_2	74

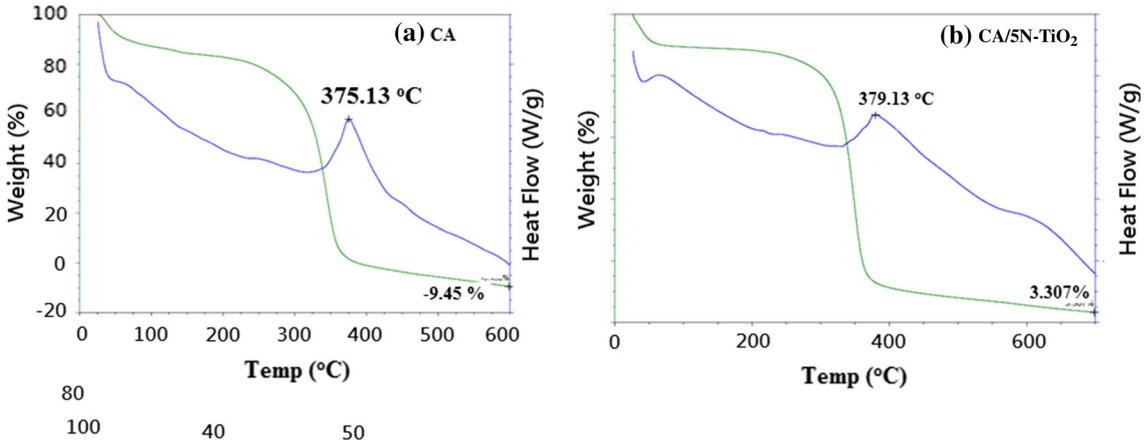

Fig. 7. TG-DSC curves of (a) CA and (b) CA/5N-TiO_2 films.

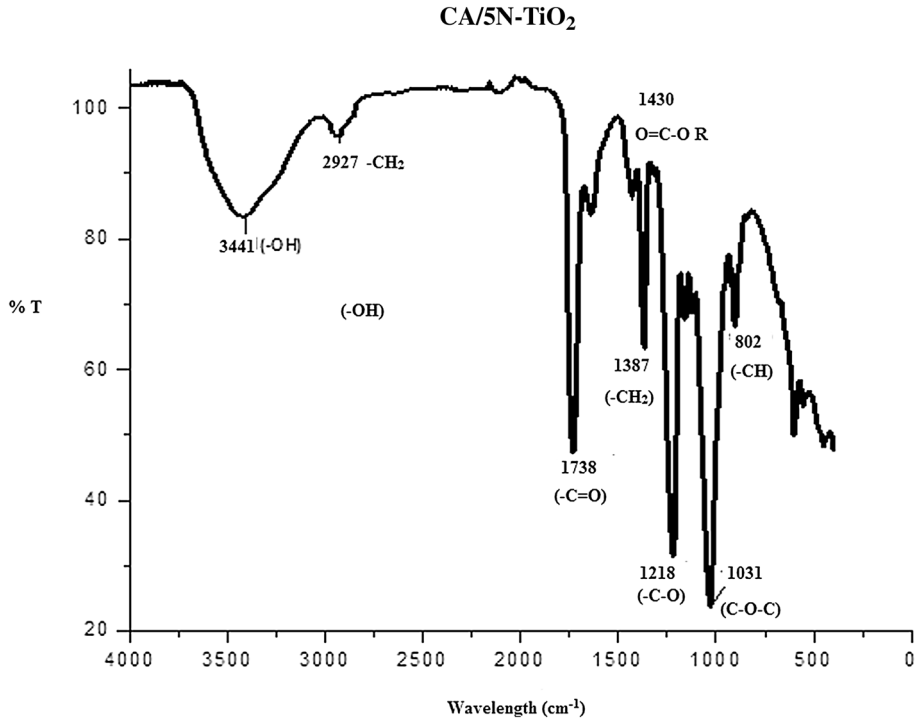

Fig. 8. FT-IR spectra of CA and CA/5N-TiO_2 films.

Characterization of CA/N-TiO_2 Photochromic Films

The flexibility and transparency of the prepared CA/N-TiO_2 films are illustrated in Fig. 5a and b, respectively. The thickness of the films was around 0.1 mm. The transmission spectra of the obtained films are presented in Fig. 6. The films exhibited high transparency (Table I); with 5 wt.% N-TiO_2 nanopowder loading, the transparency was reduced to 74% (Fig. 6). CA film showed high transparency (100%) in comparison with the nanocomposite films (Fig. 6b). In addition, the transparency of the film decreased with increasing N-TiO_2 loading. The thermal analysis results obtained for the films are shown in Fig. 7a and b. The major weight loss observed between 250°C and 300°C is due to decomposition of acetylated units of the polymer. These results show that the CA film was stable up to ~300°C and decomposed at temperature above 300°C. A similar observation was noted in the TG-DSC results for CA/5N-TiO_2 as well. FT-IR spectroscopy is mainly used as a qualitative technique to study surface chemical functional groups. Figure 8 shows the FT-IR spectra of representative systems, revealing a number of absorption bands below 2000 cm^{-1}. The major absorption features can be

attributed as follows: 1732 cm^{-1} (C=O), 1430 cm^{-1} (O=C–OR), 1367 cm^{-1} (–CH_2), 1218 cm^{-1} (C–O), 1031 cm^{-1} (C–O–C), and 902 cm^{-1} (–CH). The peaks appearing at 2927 cm^{-1} (–CH_2) and 3441 cm^{-1} (–OH) are characteristic of H_2O. Both samples exhibited similar characteristic features without introduction of any new peaks. The observation of small peaks in the region from 400 cm^{-1} to 500 cm^{-1} can be attributed to the presence of metal oxide ceramic. These results demonstrate that only physical blending rather than chemical reaction occurred between the N-TiO_2 and CA film.[13,21] A SEM micrograph of CA/5N-TiO_2 film is shown in Fig. 9, revealing uniform distribution of ceramic on the CA nanocomposite film. The surface of the film reveals the presence of ceramic.

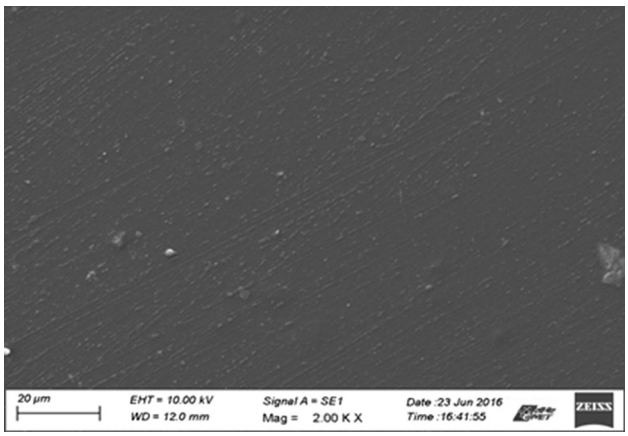

Fig. 9. SE micrograph of CA/5N-TiO_2 film.

Evaluation of Photochromic Properties of Films

The photochromic properties of the films were evaluated under UV, visible light, and simulated

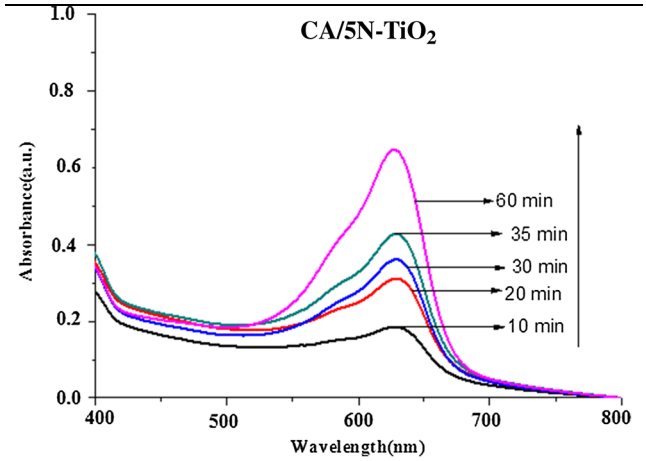

Fig. 11. UV–Vis spectra of recoloration activity of CA/5N-TiO_2 films under UV irradiation for various times.

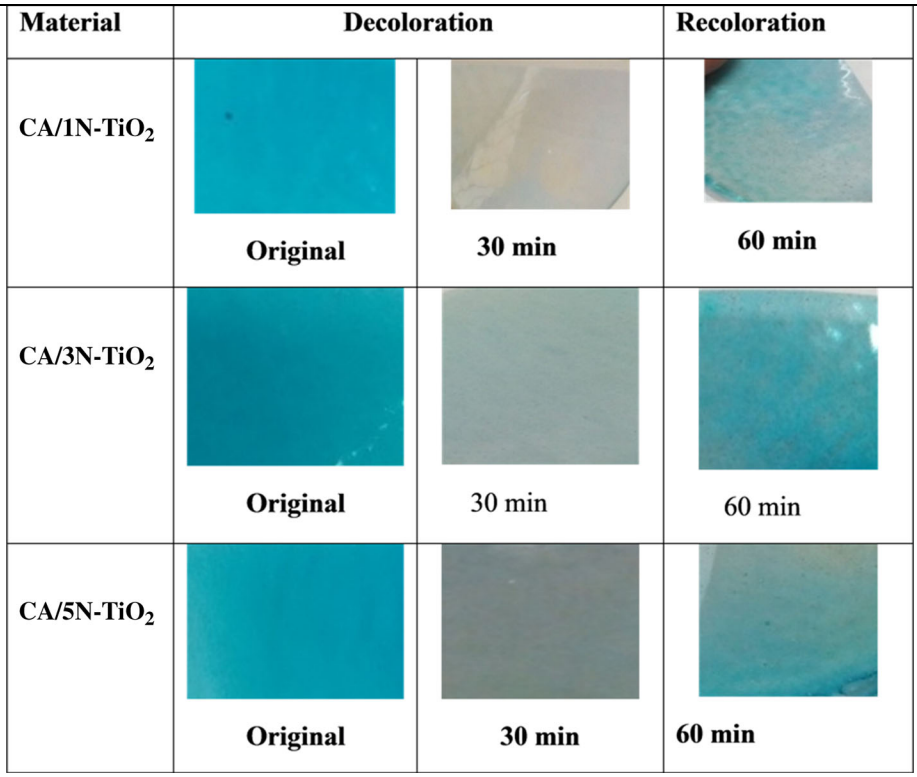

Fig. 10. Visual observation of decoloration/recoloration of biocomposite thin films under UV irradiation.

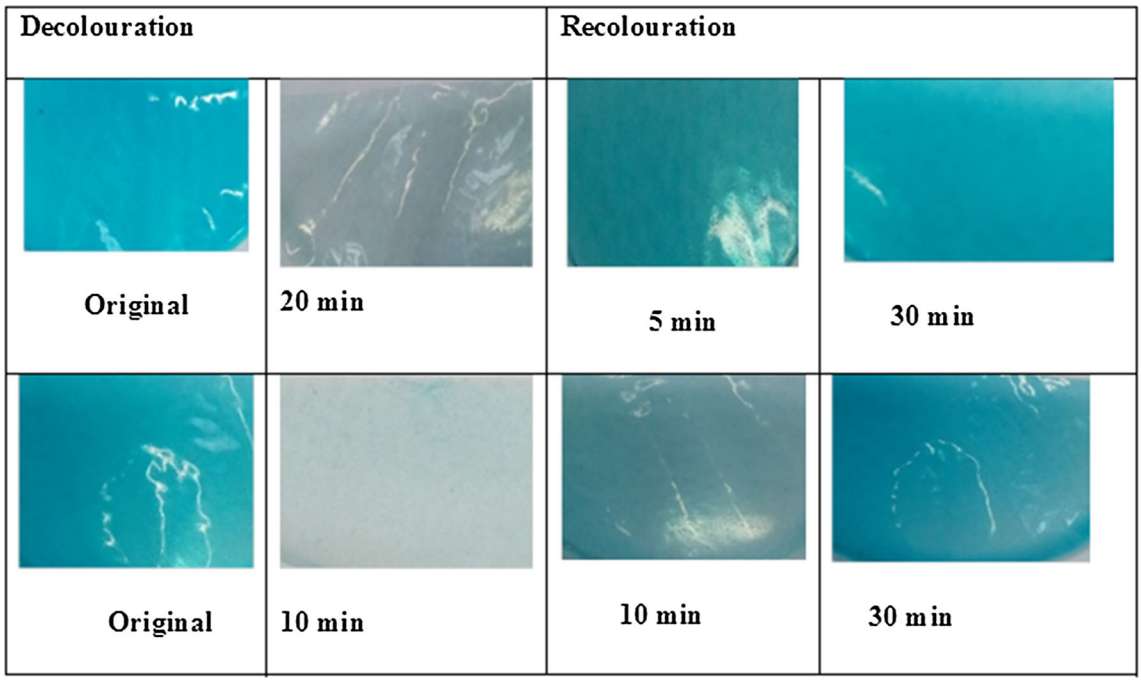

Fig. 12. Visual observation of decoloration/recoloration of biocomposite thin films under visible light irradiation.

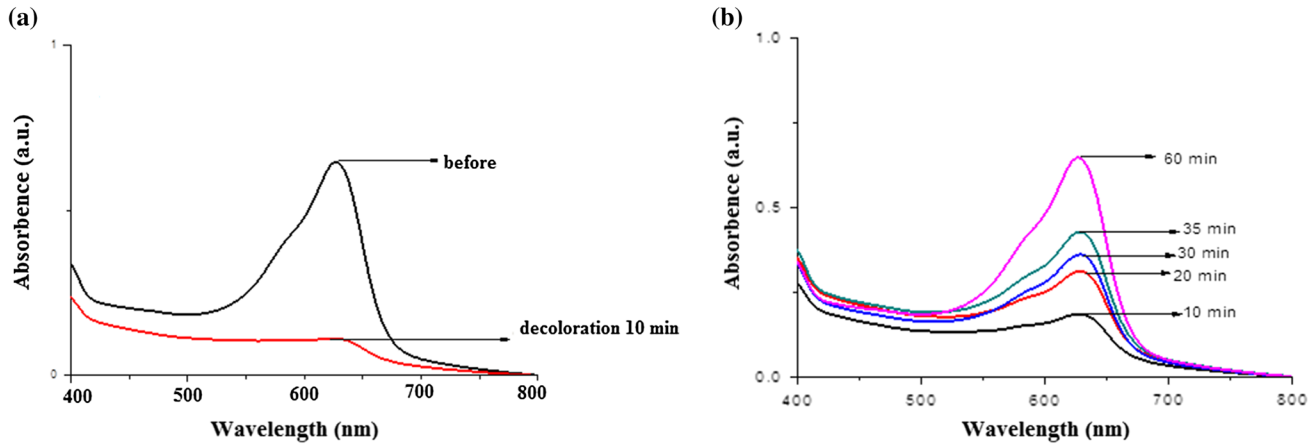

Fig. 13. UV–Vis spectra of recoloration activity under visible light irradiation for CA/5N-TiO_2 films at various times.

solar irradiation. The visual observation of the decoloration/recoloration under UV irradiation is presented in Fig. 10. The images show the results for decoloration as well as recoloration for CA films with different amounts of N-TiO_2 added. In the case of UV irradiation, complete decoloration occurred in 20 min (Fig. 10), but the recoloration process was not spontaneous, with the conversion from the colorless to colored state taking a long time. The parameters that affected the decoloration/recoloration process were (1) the intensity of the lamp used, (2) the dispersion of the N-TiO_2 nanopowder in the film, (3) the casting mode applied, and (4) the nature of the organic ink.

UV–Vis Spectroscopy Analysis

The decoloration/recoloration characteristics of the films were also studied by UV–Vis spectroscopy. The spectra obtained are shown in Fig. 11. Figure 11a shows the spectra obtained for decoloration of CA/5N-TiO_2 film under visible light irradiation. Figure 11 shows the UV–Vis spectra obtained for recoloration of CA/5N-TiO_2 film at room

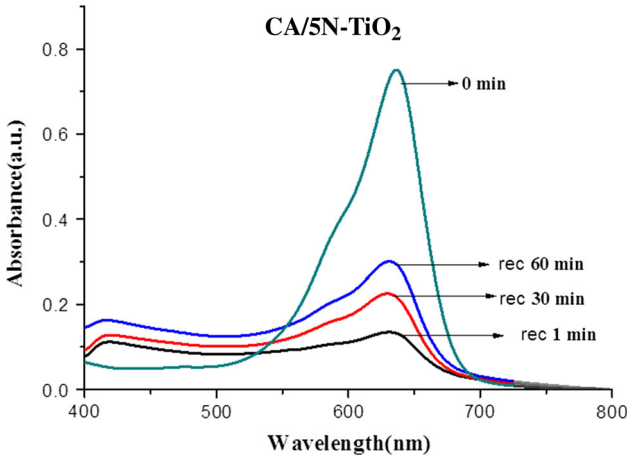

Fig. 14. UV–Vis spectra of recoloration of CA/5N-TiO_2 after irradiation with simulated solar light at various times.

temperature. The UV–Vis spectra clearly show that decoloration and recoloration of the films took place under visible light irradiation.

Photochromic Properties of Biocomposites Under Visible Light Irradiation

The films were kept under visible light irradiation for specific times and the decoloration/recoloration rate observed. Visible observations for such studies conducted with CA/5N-TiO_2 film are shown in Fig. 12. The decoloration/recoloration characteristics of the films were studied by UV–Vis spectroscopy. The spectra obtained are shown in Fig. 13a and b. Figure 13a shows the spectra obtained for decoloration of CA/5N-TiO_2 film under visible irradiation. Figure 13b shows the UV–Vis spectra obtained for recoloration of CA/5N-TiO_2 film. The UV–Vis spectral analysis confirmed the decoloration and recoloration of the films under visible light irradiation.

Photochromic Properties of Biocomposites Under Simulated Solar Irradiation

To evaluate their photochromic properties, the films were also kept under a solar simulator and analyzed by UV–Vis spectrophotometer. The decoloration/recoloration results observed for representative films are presented in Fig. 14. Under simulated solar light, the decoloration was very fast (~1 min) for CA/5N-TiO_2 film. Recoloration was almost as fast as under UV or visible light irradiation.

CONCLUSIONS

Flexible photochromic CA/N-TiO_2 nanocomposite films were fabricated using an intelligent ink and hydrothermally prepared N-TiO_2 by a simple solution casting method. Powder x-ray diffraction patterns clearly indicated that the prepared N-TiO_2 contained anatase as major phase according to JCPDS data, with crystallite size of ~20 nm. The extension of the absorbance into the visible range suggested that N-TiO_2 could enhance the photoresponse, increasing its effectiveness for applications using visible light. SEM micrographs revealed uniform morphology for the prepared ceramics and confirmed presence of N-TiO_2 in the nanocomposite. These as-prepared biopolymer–nanocomposite flexible films exhibit unique properties for specific applications. This fabrication strategy provides insight into the potential use of green chemistry-based biopolymer–nanocomposite materials for various photochromic applications in the future.

ACKNOWLEDGEMENTS

R.J.R. and H.A.A. are grateful to the Deanship of Scientific Research, King Saud University for funding through the Vice Deanship of Scientific Research Chair.

REFERENCES

1. M. Nogi and H. Yano, *Adv. Mater.* 20, 1849 (2008).
2. T. Abitbol, A. Rivkin, Y. Cao, Y. Nevo, E. Abraham, T. Ben-Shalom, S. Lapidot, and O. Shoseyov, *Curr. Opin. Biotechnol.* 39, 76 (2016).
3. M. Biancardo, R. Argazzi, and C.A. Bignozzi, *Inorg. Chem.* 44, 9619 (2005).
4. W. Wang, N. Xie, L. He, and Y. Yin, *Nat. Commun.* 5, 5459 (2014).
5. S.M.A.S. Keshk, M.S. Hamdy, and I.H.A. Badr, *Am. J. Polym. Sci.* 5, 24 (2015).
6. H. Kato, K. Asakura, and A. Kudo, *J. Am. Chem. Soc.* 125, 3082 (2003).
7. O.L. Galkina, K. Onneby, P. Huang, V.K. Ivanov, A.V. Agafonov, G.A. Seisenbaeva, and V.G. Kessler, *J. Mater. Chem. B* 3, 7125 (2015).
8. B. Naik, S. Martha, and K.M. Parida, *Int. Hydrog. Energy* 36, 2794 (2011).
9. J. Jang, H.S. Lee, and W.S. Lyoo, *Fibers Polym.* 8, 19 (2007).
10. A.W. Morawski, E. Nejman, J. Przepiorski, R. Kordala, and J. Pernak, *Cellulose* 20, 1293 (2013).
11. S.D. Wang, Q. Ma, H. Liu, K. Wang, L.Z. Ling, and K.Q. Zhang, *Adv. Mater.* 5, 40521 (2015).
12. A. Mills, J. Wang, S.K. Lee, and M. Simonsen, Chem. Comm. (2005). doi:10.1039/b501131k.
13. X. Jin, J. Xu, X. Wang, Z. Xie, Z. Liu, B. Liang, D. Chen, and G. Shen, *Adv. Mater.* 4, 12640 (2014).
14. R. Dholam, N. Patel, A. Adami, and A. Miotello, *Int. J. Hydrog. Energy* 34, 5337 (2009).
15. T.C. Hong, T. Radhika, R.J. Ramalingam, and F. Adam, *Synth. React. Inorg. Metal-Org. Nano-Metal Chem.* 46, 741 (2016).
16. W. Wang, M. Ye, L. He, and Y. Yin, *Nano Lett.* 14, 1681 (2014).
17. A. Mills and D. Hazafy, *Analyst* 133, 213 (2008).
18. T. Ohsaka, F. Izumi, and Y. Fujiki, *J. Raman Spectrosc.* 7, 321 (1978).
19. M.H. Razali, A.M.N. Fauzi, A.R. Mohamed, and S. Sreekantan, *Int. J. Mater. Mech. Manuf.* 1, 314 (2013).
20. A.L. Castro, M.R. Carvalho, M.D. Ferreira, and L.P. Jumas, *J. Solid State Chem.* 182, 1838 (2009).
21. J. Jang, H.S. Lee, and W.S. Lyoo, *Fibers Polym.* 8, 19 (2007).